Magnetocrystalline anisotropy in (111) $CoPt_3$ thin films probed by x-ray magnetic circular dichroism

W. Grange, M. Maret, and J.-P Kappler
Institut de Physique et de Chimie des Matériaux de Strasbourg (IPCMS), 23 rue du Loess, 67037 Strasbourg Cedex, France

J. Vogel and A. Fontaine
Laboratoire de Magnétisme Louis Néel, CNRS, B.P. 166, 38042 Grenoble, France

F. Petroff
Unité Mixte CNRS-Thomson CSF, Domaine de Corbeville, 91404 Orsay, France

G. Krill
Laboratoire pour l'Utilisation du Rayonnement Electromagnétique (LURE), Bâtiment 209D, 91405 Orsay, France

A. Rogalev, J. Goulon, M. Finazzi, and N. B. Brookes
European Synchrotron Radiation Facility (ESRF), B.P. 220, 38043 Grenoble Cedex, France
(Received 20 February 1998)

Angle-dependent x-ray magnetic circular dichroism experiments have been performed at both the Co and Pt $L_{2,3}$ edges in two epitaxial (111) $CoPt_3$ thin films grown at 690 and 800 K. The analysis of the angular variations of the $3d$ orbital magnetic moment shows two different magnetic behaviors: a strong perpendicular magnetocrystalline anisotropy (PMA) for the film grown at 690 K and an almost isotropic behavior for the film grown at higher temperature. The same analysis at the Pt $L_{2,3}$ edges suggests that the $5d$ electrons play an important role in the PMA. Our results correlate the appearance of PMA with the existence of anisotropic structural effects induced during the codeposition process. [S0163-1829(98)07534-1]

I. INTRODUCTION

Recently, ultrahigh-vacuum preparation methods such as molecular beam epitaxy (MBE) have been appealing routes to fabricate new materials for short-wavelength magneto-optic (MO) recording. In this respect, Co/Pt or Co/Pd multilayers, which may exhibit strong perpendicular magnetocrystalline anisotropy (PMA) and a large Kerr rotation at short wavelengths, have been extensively studied.[1–3] Co-evaporated Co-Pt thin films have also shown strong PMA with 100% remanence and enhanced MO signals with respect to Co/Pt multilayers.[4] In epitaxial $CoPt_3$ thin films, PMA was clearly shown to be dependent on the growth temperature.[5,6] Strong PMA (unexpected for a cubic lattice) was observed in films coevaporated around 690 K and was related to the existence of anisotropic chemical local order (yielding the formation of microscopic Co-rich and Co-poor planar local regions).[7,8] In contrast, films grown below 500 K and above 800 K present no PMA. These changes were correlated to their isotropic fcc structure which is disordered and ordered $L1_2$ type, respectively. Such changes in chemical local ordering would result from (i) the competition between surface and bulk diffusion and (ii) the tendency of Pt atoms to segregate at the advancing free surface during growth. At 690 K, surface diffusion is the dominant diffusion process and the atomic arrangements (i.e., the formation of these microscopic Co-rich and Co-poor regions) built at the growth surface are simply frozen; at 800 K enhanced bulk diffusion tends to destroy them, favoring the formation of the $L1_2$-type equilibrium phase, and below 500 K surface diffusion is too weak.[6] In these alloy films, the correlation between PMA and the structural state has been established either by magnetization loops or torque measurements. Both methods are not element specific, cannot distinguish between the shape anisotropy and the magnetocrystalline anisotropy (MCA), and characterize MCA in terms of phenomenological anisotropy energy constants.

In 1995, angle-dependent x-ray magnetic circular dichroism (XMCD) measurements performed by Weller *et al.*[9] have provided direct experimental support for the tight-binding approach of MCA proposed by Bruno[10] and refined recently by van der Laan.[11] In this model based on a perturbation treatment, Bruno shows a direct connection between MCA and the anisotropy of the orbital magnetic moment. In this respect, we emphasize that XMCD is certainly the most direct and sensitive technique to provide a quantitative information on MCA through separate spin and orbital magnetic moment evaluations on specific shells and sites.[12,13]

In this work, we present high-field angle-dependent XMCD measurements performed at both the Co and Pt $L_{2,3}$ edges in two fcc (111) $CoPt_3$ thin films (grown at 690 and 800 K). These two films can be viewed as model systems for our study since they present a large difference in MCA. An anisotropy of the $3d$ orbital magnetic moment as high as $0.13\mu_B$ (per Co atom) is observed for a film grown at 690 K, whereas no significant variation is found for a film grown at higher temperature. The measurements performed at the Pt $L_{2,3}$ edges show the same trends. These results correlate the anisotropic short-range chemical order with the appearance of MCA and emphasize the role of the Pt atoms in the MCA.

 © 1998 The American Physical Society

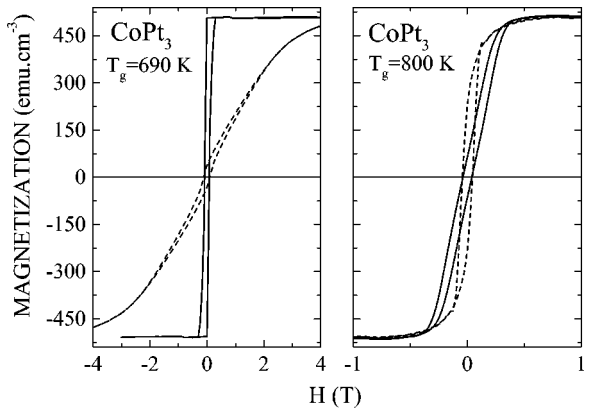

FIG. 1. Superconducting quantum interference device (SQUID) hysteresis magnetic loops for two epitaxial (111) $CoPt_3$ thin films measured at 30 K with the field applied parallel (dashed line) and perpendicular (solid line) to the film plane. Left panel: film grown at 690 K. Right panel: film grown at 800 K.

II. SAMPLE PREPARATION AND CHARACTERIZATION

(111) $CoPt_3$ thin films were deposited at 690 and 800 K under UHV conditions on a mica (0001) substrate, following the growth of a 15-nm Ru (0001) buffer layer grown at 900 K.[6] The 50-nm-thick films were then covered by a 1.5-nm Pt layer to prevent oxidation. The deposition rates of Co and Pt, monitored by two quartz balances, were 0.005 and 0.020 nm/s, respectively. The structural characterization was performed *in situ* by a reflection high-energy electron-diffraction (RHEED) analysis and *ex situ* by x-ray diffraction (XRD).[6] The RHEED patterns observed along the azimuths $[10\bar{1}0]$ and $[11\bar{2}0]$ of Ru revealed the high quality of our (111) epitaxial films on the Ru buffer. The XRD measurements performed on a high-resolution x-ray Philips diffractometer using Cu $K\alpha$ radiation confirmed the fcc-type stacking, with a lattice parameter a_{fcc} equal to 0.3852 and 0.3831 nm for the films grown at 690 and 800 K, respectively. Based on the composition dependence of the lattice parameter in the fcc CoPt bulk alloys, the corresponding platinum composition is equal to 75% and 68%, respectively. Complementary XRD measurements in transmission were carried out at the French synchrotron facility, LURE, below the Co *K* absorption edge. These measurements show a long-range chemical $L1_2$-type ordering only for the film grown at 800 K. The absence of such ordering for the film grown at 690 K indicates that the alloy is chemically disordered in the fcc lattice.

Before giving more details about the structure of the films, we show in Fig. 1 the magnetization hysteresis loops. The film grown at 690 K exhibits a strong PMA whereas the film grown at 800 K presents an almost isotropic behavior. These results suggest the existence of anisotropic local order effects in the film grown at 690 K, which were confirmed by polarized x-ray-absorption fine structure (XAFS) measurements. The analysis of the XAFS spectra performed at the Co *K* and Pt L_3 edges has shown preferential Co-Pt pairs together with a decrease of Pt-Pt pairs, when changing from in-plane to out-of-plane polarization.[7] As already outlined, the existence of such a chemically anisotropic short-range order is the consequence of a dominant surface diffusion associated with a Pt segregation along the advancing surface during growth. Therefore, the film grown at 690 K may be seen as a stacking of alternating Pt-rich and Pt-Co planar local regions along the growth direction. The growth temperature that determines the dominant process between surface and bulk diffusion is the key parameter to obtain such a microstructure.[6]

III. EXPERIMENTAL DETAILS

X-ray-absorption spectra (XAS) were measured at the European Synchrotron Radiation Facility (ESRF) in Grenoble (France) on the ID12A (Pt $L_{2,3}$ edges) and ID12B (Co $L_{2,3}$ edges) beamlines. The straight section ID12 is equipped with two undulators, Helios-I and Helios-II, that cover an energy range from soft (0.5–1.6 keV) to hard (3–22 keV) x rays, respectively.[14] These beam lines have been specially designed for polarization-dependent x-ray-absorption spectroscopy studies: by longitudinal phasing of the undulator magnetic arrays, either linear or circular polarization can be easily obtained. For the experiments performed at the Pt $L_{2,3}$ edges, the third harmonic of the undulator Helios-II was chosen and a double-Si(111)-crystal monochromator ensured the monochromatization of the beam. At the Co $L_{2,3}$ edges, the monochromatic beam was supplied by a grating spectrometer. Note that the intense circular polarized radiation emitted by both undulators is very well transferred by the optical elements: the polarization rate is estimated to be 0.9 (Pt $L_{2,3}$ edges) and 0.85 (Ref. 15) (Co $L_{2,3}$ edges), respectively.

The XAS spectra were monitoring at room temperature in the total fluorescence yield (TFY) detection mode at the Pt $L_{2,3}$ edges and in the total electron yield (TEY) detection mode at the Co $L_{2,3}$ edges. The XMCD signal was obtained by reversing the direction of the 4-T applied magnetic field, keeping the helicity of the incoming beam fixed. For both experiments, the direction of the magnetic field generated by a superconducting magnet was parallel to the direction of the incoming beam. In the following discussion, γ will denote the angle between the direction of the incident photon beam and the normal to the surface (i.e., the [111] direction).

Finally, we emphasize that the experiments performed at the Pt $L_{2,3}$ edges are very challenging since the absorption coefficient of a 50-nm $CoPt_3$ film is only about 0.03.

IV. RESULTS

The most direct method for measuring the absorption cross section is the transmission technique. For epitaxial films deposited on thick or opaque substrates, alternative techniques such as fluorescence (FY) or electron yield (EY) techniques have, however, to be used.[16,17] The FY technique presents an advantage over the EY technique owing to its bulk sensitivity and the possibility to apply strong magnetic fields. Since these two techniques measure the decay of the core hole created in the absorption, they give an indirect measure of the absorption cross section. Assuming a proportionality between FY (EY) and the absorption coefficient requires therefore a thorough analysis.

Some of the main difficulties encountered in the FY measurements consist of self-absorption effects, leading to a distortion of the absorption spectra.[18] It is worth noting that such effects are not observed for dilute species or when the

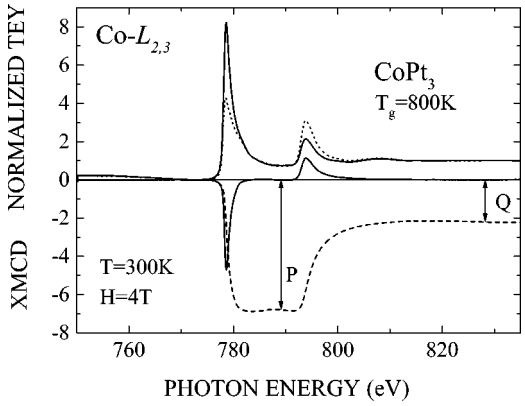

FIG. 2. Co $L_{2,3}$ absorption spectra of $CoPt_3$ thin film (grown at 800 K) recorded with parallel (dots) and antiparallel (solid line) alignment of the direction of the incoming x rays and the magnetization vector. For this experiment, the direction of the 4-T applied magnetic field was parallel to the surface normal. The corresponding XMCD signal (corrected for the incomplete polarization of the x rays) and its integration (dashed line) are also presented. The *P* and *Q* are the integrals needed in the sum rules.

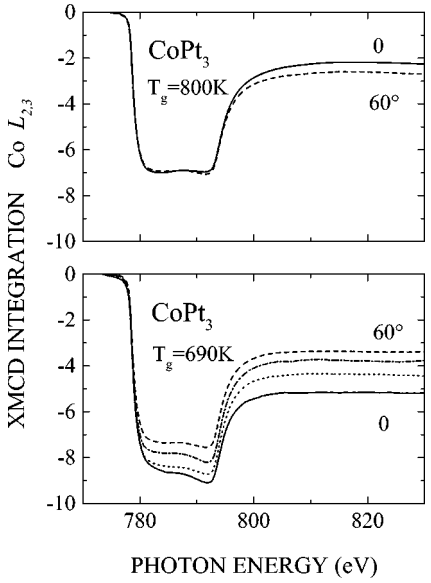

FIG. 3. Integrated dichroism signal (corrected for the incomplete polarization of the x rays) at the Co $L_{2,3}$ edges measured for different incidence angle γ in the two $CoPt_3$ thin films ($H=4$ T, $T=300$ K). Upper panel: thin film grown at 800 K ($\gamma=0$, solid line; $\gamma=60°$, dashed line). Lower panel: thin film grown at 690 K ($\gamma=0$, solid line; $\gamma=15°$, dots; $\gamma=45°$, short dashed line; $\gamma=60°$, dashed line).

penetration depth of the incoming photons is large with respect to the thickness of the film. At the Pt $L_{2,3}$ edges, the transmission coefficient is about 0.97 for a 50-nm $CoPt_3$ film and no sizable self-absorption effects are observed. At the Co $L_{2,3}$ edges, the penetration depth of the incoming x rays is only about a few hundred angstrom. We consequently perform the measurements in the EY mode, restricting our analysis to $\gamma<60°$, since the EY also suffers from saturation effects at glancing angles.[19,20]

Finally, we mention that the multiplet effects reported by de Groot *et al.*[21] in the FY measurements are expected to be small at the Pt $L_{2,3}$ edges since the absorption process ($2p\rightarrow 5d$) is not resonant with the main fluorescence process ($3d\rightarrow 2p$).

A. XMCD at the Co $L_{2,3}$ edges

Figure 2 shows typical Co $L_{2,3}$-edge XAS spectra (and the corresponding XMCD signal corrected for the incomplete polarization of the x rays) measured with the field applied parallel and antiparallel to the direction of the incoming beam. The experimental XAS spectra were normalized such that the Co L-edge jump is equal to 1. Although XMCD is strictly defined as the difference in absorption for right and left circular polarized light, we recall that—in the electric dipole approximation—inverting the applied magnetic field or the circular polarization gives the same results.[22] Using the notations of Arvanitis *et al.*,[23] the angle-dependent orbital sum rule for XMCD takes the following form:

$$m_{orb}^{\gamma}=-(2Q^{\gamma}/3R)(10-n_{3d}), \tag{1}$$

where m_{orb}^{γ} denotes the orbital magnetic moment measured at the angle γ, Q^{γ} is the integrated dichroism intensity over the L_3 and L_2 edges at the angle γ, R is the $3d$ isotropic absorption cross section, and n_{3d} is the number of electrons in the $3d$ shell. To separate the transitions to unoccupied $3d$ states (the ''white line'') from the continuum, a simple steplike function was subtracted from the isotropic absorption cross section.

For all measurements, the 4-T applied magnetic field was large enough to saturate the total magnetic moment. Therefore no additional data corrections are needed. For the thin film grown at 690 K, the incidence angle was varied from 0 to 60° (every 15°), whereas only two measurements were performed for the film grown at 800 K (0 and 60°).

Figure 3 shows the result of the integrated dichroism intensity for the two samples (corrected for the degree of circular polarization of the x rays). As already outlined, an angle dependence of Q, and consequently in the orbital magnetic moment, when the spins are forced out of the [111] direction by the applied magnetic field, is the signature of MCA. For the film grown at 800 K, only a small variation is found in the orbital magnetic moment, with an in-plane component slightly larger than the out-of-plane component. These results are inverted from those found for the film grown at 690 K: in this case, the orbital magnetic moment is strongly anisotropic and now oriented along the normal to the surface. Assuming uniaxial anisotropy, we can compare our experimental data with the model of Bruno who suggests that the $3d$ orbital magnetic moment varies (at lowest order) as $m_{orb}^{\gamma}=m_{orb}^{\perp}+(m_{orb}^{//}-m_{orb}^{\perp})\sin^2\gamma$, where $m_{orb}^{\perp}$ and $m_{orb}^{//}$ denote, respectively, the orbital magnetic moment measured along and perpendicular to the easy axis of magnetization.[10] Figure 4 shows the good agreement between our experimental results and the theoretical prediction, supporting the present model. Taking into account the number of electrons in the $3d$ shell (7.75),[24] we found $m_{orb}^{\perp}=(0.30\pm 0.02)\mu_B$ and $(m_{orb}^{\perp}-m_{orb}^{//})=(0.13\pm 0.02)\mu_B$, per Co atom.

The difference in the anisotropy of the orbital magnetic moment between the films grown at 690 and 800 K (given in

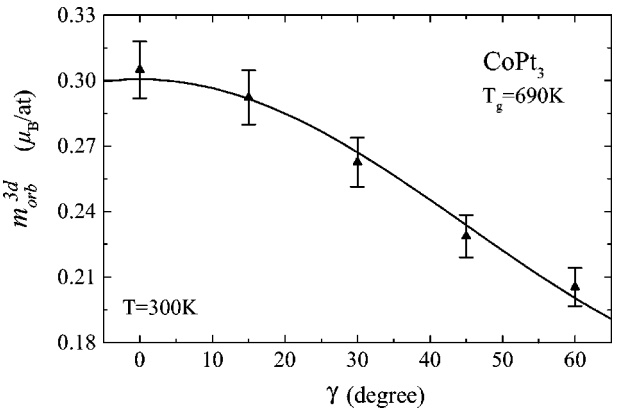

FIG. 4. $3d$ orbital magnetic moment (in units of μ_B/atom), measured in the (111) $CoPt_3$ thin film grown at 690 K, as a function of the photon incidence angle γ ($H=4$ T, $T=300$ K). The solid curve is a fit assuming that the $3d$ orbital magnetic moment varies as $m^{\gamma}_{orb}=m^{\perp}_{orb}+(m^{//}_{orb}-m^{\perp}_{orb})\sin^2\gamma$, where $m^{\perp}_{orb}$ and $m^{//}_{orb}$ denote, respectively, the orbital magnetic moment measured along and perpendicular to the easy axis of magnetization (i.e., the [111] direction for the film grown at 690 K).

Table I) is consistent with the macroscopic magnetization measurements (Fig. 1). Indeed, the shape of the magnetization hysteresis loop shows (i) a large PMA for the film grown at 690 K (Ref. 25) and (ii) an almost isotropic behavior for the film grown at 800 K. Note that the magnetization curves obtained for the film grown at 800 K suggest that the magnetization lies in plane, in agreement with our XMCD results.

Moreover, our results are well correlated with the difference in the structural order. At 690 K, the dominant surface diffusion process coupled with the segregation of Pt at the growth surface produces the formation of preferential Co-Pt pairs along the growth direction (i.e., the [111] direction) and consequently an important broadening in the band structure along this direction. As compared to the film grown at 800K, the orbital magnetic moment in the film grown at 690 K will be greatly enhanced along the [111] direction and therefore be strongly anisotropic.[26,27]

The major interest of XMCD sum rules is the possibility to determine separately the orbit and spin contributions from the total magnetic moment. Using the same notation as in Eq. (1), the angle-dependent spin sum rule is written as

$$m_{spin}-7m^{\gamma}_{T}=-\frac{(3P^{\gamma}-2Q^{\gamma})(10-n_{3d})}{R}, \qquad (2)$$

TABLE I. The Co orbital magnetic moment (along the normal to the surface) and its anisotropy $\Delta m^{3d}_{orb}=(m^{\perp}_{orb}-m^{//}_{orb})$ (in units of μ_B/atom) measured in the two studied (111) $CoPt_3$ thin films ($m^{\perp}_{orb}$ and $m^{//}_{orb}$ denote, respectively, the orbital magnetic moment measured along and perpendicular to the easy axis of magnetization). Note that the easy direction of magnetization lies in plane for the film grown at 800 K (see Fig. 3).

	m^{3d}_{orb} (± 0.02)	Δm^{3d}_{orb} (± 0.02)
$CoPt_3$ ($T_g=690$ K)	0.30	0.13
$CoPt_3$ ($T_g=800$ K)	0.15	0.02

where m_{spin} denotes the spin magnetic moment,[28] m^{γ}_{T} is the magnetic dipole term measured at the angle γ, and P^{γ} is the dichroism intensity over the L_3 edge at the angle γ.

The magnetic dipole term arises from the anisotropy of the spin density within the Wigner-Seitz cell[13] and can therefore represent a significant contribution to the effective spin magnetic moment $m^{\gamma}_{eff\ spin}=m_{spin}-7m^{\gamma}_{T}$ (i.e., the quantity directly determined by applying the spin sum rule) for a low-symmetry crystal environment or high spin-orbit splitting.[29] For $3d$ metals, Wu and Freeman[29] have shown that the use of the spin sum rule results in an error up to 50% rule for the (001) surface of Ni. In agreement with previous experimental studies,[30] they found, however, that the magnetic dipole term could be safety neglected in the case of cubic symmetry. Thus, for the film grown at 800 K with a $L1_2$-type long-range chemical ordering, neglecting m^{γ}_{T} in the spin sum rule is certainly a good approximation. Using a $3d$ occupation number of 7.75,[24] we obtain $m_{spin}=(1.60\pm 0.10)\mu_B$ per Co atom.

With regard to the large orbital moment anisotropy found in the film grown at 690 K, the magnetic dipole term should be now more significant. This is confirmed by the variation of the effective spin magnetic moment itself: we obtain $m_{eff\ spin}=(1.58\pm 0.10)\mu_B$ and $m_{eff\ spin}=(1.40\pm 0.10)\mu_B$ for $\gamma=15°$ and $\gamma=60°$, respectively. To determine separately the spin and magnetic dipole contributions to the effective spin moment, we follow the arguments of Stöhr and König.[31] In $3d$ transition metals, the effect of the spin-orbit interaction on the magnetic dipole term is weak; therefore, for a uniaxial anisotropy, we can write $m^{\perp}_{T}+2m^{//}_{T}=0$, where $m^{\perp}_{T}$ and $m^{//}_{T}$ denote, respectively, the dipole magnetic moment measured along and perpendicular to the easy axis of magnetization. Since the magnetic dipole term, similarly to the orbital magnetic moment, is expected to vary as $m^{\gamma}_{T}=m^{\perp}_{T}+(m^{//}_{T}-m^{\perp}_{T})\sin^2\gamma$ (in the absence of in-plane anisotropy), the effective spin magnetic moment should vary as $m^{\gamma}_{eff\ spin}=\lambda+\beta\ \sin^2\gamma$, where $\lambda=(m_{spin}-7m^{\perp}_{T})$ and $\beta=\frac{21}{2}m^{\perp}_{T}$. We derive a spin magnetic moment per Co atom equal to $(1.44\pm 0.10)\mu_B$ and a magnetic dipole term m_T of $-(0.019\pm 0.003)\mu_B$ and $(0.009\pm 0.002)\mu_B$ for the out-of-plane and in-plane orientations, respectively.

Although the orbital magnetic moment is enhanced by a factor of about 2 in the film grown at 690 K (see Table I), the spin magnetic moment does not show a significant variation for the two samples. This result is consistent with previous studies that have clearly pointed out that the Co spin magnetic moment is less sensitive to changes in atomic environment.[26,32]

B. XMCD at the Pt $L_{2,3}$ edges

According to calculations, the strong MCA observed in Co-Pt or Co-Pd systems results mainly from the nonmagnetic element.[33,34] Due to their strong spin-orbit coupling, the $5d$ ($4d$) states acquire a sizable orbital polarization [once a spin polarization is induced by the strong $5d(4d)$-$3d$ hybridization] and therefore give an important contribution to the MCA. In a naive picture, the $3d$ electrons would play a minor role in the MCA, acting only as a ''source of magnetism.'' To pursue the understanding of the appearance of MCA in Co-Pt systems, we present in this section angle-

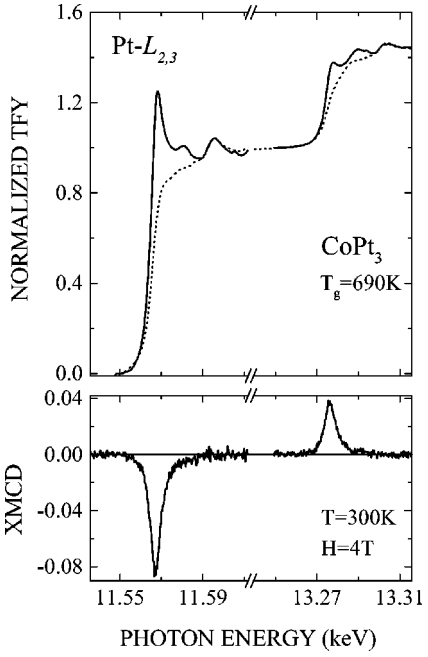

FIG. 5. Upper panel: typical $L_{2,3}$ isotropic absorption edges of Pt in the (111) $CoPt_3$ thin film grown at 690 K (solid curve) and those of Au in a $CuAu_3$ bulk sample (dots) for $\gamma=30°$. Lower panel: XMCD signal at the Pt $L_{2,3}$ edges corrected for the circular polarization rate ($H=4$ T, $T=300$ K).

dependent XMCD measurements at the Pt $L_{2,3}$ edges on the $CoPt_3$ thin films under study. The incident angle γ was varied from 10° to 60° (10°, 30°, 45°, 60°) for the thin film grown at 690 K and two measurements were performed for the film grown at 800 K (30° and 80°).

To our knowledge, only few XMCD experiments have been performed at the Pt $L_{2,3}$ edges since the measurements of Shütz *et al.* in 1989.[35] For example, Maruyama *et al.* have presented some results concerning the induced Pt magnetic moments in TM-Pt_3 (TM=Cr, Mn, Co) bulk alloys.[36,37] While the analysis of Pt XMCD spectra requires some care, only few details have been given in these previous studies. To address this properly, we give in the following discussion more details and argue that a rough analysis could lead to large errors in the determination of the $5d$ spin and orbital magnetic moments.

Figure 5 shows a normalized Pt isotropic absorption spectrum and the corresponding XMCD signal for the thin film grown at 690 K ($\gamma=30°$). The XMCD signal is corrected for the incomplete polarization of the x rays. As outlined by Mattheiss and Dietz,[38] an important feature of the $L_{2,3}$ absorption spectra of Pt is that the ratio of the L_3 to L_2 edge jumps, r_L, deviates from the statistical ratio (i.e., the ratio corresponding to the degeneracy of the core-hole states). They have experimentally found $r_L=2.22$ in pure Pt and have attributed this effect to a difference between the $R^{2p_{1/2}}$ and $R^{2p_{3/2}}$ radial functions. To account for this effect, we thus normalize the XAS spectra recorded in the TFY detection mode by adjusting the step height ratio to 2.22. This procedure is far from insignificant since the radial integrals in the sum rules are supposed to be independent of both the energy and the spin direction. We however check that correcting the sum rules for this effect [for example in Eq. (2), substitute $(3.22P^{\gamma}-2.22Q^{\gamma})$ for $(3P^{\gamma}-2Q^{\gamma})$] results in a discrepancy in the value of the orbital and spin magnetic moment lower than 10%. Note that this discrepancy is comparable to the precision of our measurements.

To separate the transitions to unoccupied $5d$ states from the continuum $(2p\rightarrow nd,s)$, a steplike function (or an arctangent curve) is generally subtracted from the isotropic absorption cross section. This procedure has been extensively used for the determination of the $3d$ near-edge resonance. However, the L_3 and L_2 Pt edges do not exhibit a strong ''white line'' and the errors in the determination of the steplike background, negligible at the Co $L_{2,3}$ edges, might now be as large as 40%. For an accurate analysis, we have therefore compared the L_3 and L_2 Pt edges with those of Au, measured under the same experimental conditions in a $CuAu_3$ bulk sample. The energy scale of the Au spectra was expanded by a factor of 1.07 to account for the difference in the lattice parameter, then aligned in energy with the Pt spectra on the fine structure and finally normalized to the edge jump.[39]

According to this procedure the isotropic absorption cross section per $5d$ holes is

$$\frac{R}{(10-n_{5d})}=\int_{L_{2,3}}\frac{d\omega}{\omega}\left(\frac{\sigma_{tot}^{\mathrm{Pt}}(\omega)-\sigma_{tot}^{\mathrm{Au}}(\omega)}{(n_{5d}^{\mathrm{Au}}-n_{5d}^{\mathrm{Pt}})}\right), \qquad (3)$$

where $\int_{L_{2,3}}(d\omega/\omega)[\sigma_{tot}^{\mathrm{Pt}}(\omega)-\sigma_{tot}^{\mathrm{Au}}(\omega)]$ is the integrated intensity of the difference between the isotropic Pt and Au

TABLE II. The Pt orbital and spin magnetic moments (in units of μ_B/atom) measured in the two studied (111) $CoPt_3$ thin films. Also the ratio $m_{orb}^{5d}/m_{spin}^{5d}$ is given for a more accurate analysis. We assume that the contribution of the magnetic dipole term to the effective spin magnetic moment is negligible.

		$CoPt_3$ ($T_g=690$ K)	
γ (degree)	m_{orb}^{5d} (±0.004)	m_{spin}^{5d} (±0.02)	$m_{orb}^{5d}/m_{spin}^{5d}$ (±0.02)
10	0.058	0.22	0.26
30	0.052	0.23	0.22
45	0.049	0.22	0.22
60	0.044	0.24	0.18
		$CoPt_3$ ($T_g=800$ K)	
γ (degree)	m_{orb}^{5d} (±0.005)	m_{spin}^{5d} (±0.03)	$m_{orb}^{5d}/m_{spin}^{5d}$($\pm0.03$)
30	0.053	0.23	0.23
80	0.057	0.24	0.24

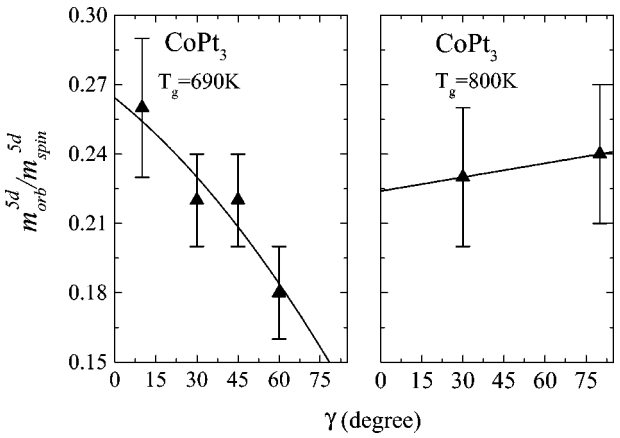

FIG. 6. The angular dependence of the m_{orb}/m_{spin} ratio of Pt atoms for two (111) $CoPt_3$ thin films grown at 690 K (left panel) and 800 K (right panel). We assume that the contribution of magnetic dipole term to the effective spin magnetic moment is negligible. The solid lines are guides for the eyes.

normalized absorption cross section (i.e., the cross section divided by the photon energy) over the L_3 and L_2 edges and $(n_{5d}^{\mathrm{Au}}-n_{5d}^{\mathrm{Pt}})$ is the electron number difference estimated to be 1.06.[24]

Table II reports the values of the orbital and spin magnetic moments determined from the application of the sum rules [Eqs. (1) and (2)] for the film grown at 690 K (the values have been corrected for both the degree of circular polarization and the fraction of nonmagnetic Pt atoms in the protective top layer). Also the ratio m_{orb}/m_{spin}, which does not depend on both the renormalization factor and the degree of circular polarization, is given for a more accurate analysis. We have assumed that the contribution of the magnetic dipole term to the effective spin magnetic moment is negligible due to the important $5d$ band broadening.[30,39]

In agreement with band structure calculations,[34] we find a strong orbital polarization (about 25% of the spin moment). Moreover, the ratio of the orbital to spin magnetic moment decreases when the spins are forced out of the [111] direction by the external magnetic field. The importance of the present result is that it provides direct experimental evidence of the role played by the $5d$ electrons in the MCA. Since the spin-orbit interaction of the Pt atoms is about 8 times larger than that of Co, the relative small variation of the Pt orbital magnetic moment plays, however, an important, if not crucial, role in the appearance of PMA.

Let us now turn to the $CoPt_3$ sample grown at 800 K (Fig. 6 and Table II). The ratio of the orbital to spin magnetic moment is now roughly isotropic, as already observed for the $3d$ electrons. This isotropy should be obviously correlated to the formation of the $L1_2$-type ordering in this film.

Interestingly, the absolute value of the orbital magnetic moment measured along the easy direction of magnetization is the sames for the samples grown at 690 and 800 K (Table II). This differs with previous studies that have found a direct connection between the enhancement of the orbital moment and the appearance of MCA in thin films.[40] The reason should be ascribed to the formation of the Pt segregation in the film grown at 690 K. In such Pt-enriched regions, the reduced number of Co magnetic neighbors has a strong impact on the spin polarization of the Pt atoms. We therefore still measure an anisotropy, but the absolute value of the orbital magnetic moment is strongly reduced since, on average, fewer Pt atoms contribute to the total Pt magnetic moment. These results are in agreement with both theoretical[41] and experimental studies:[42] By means of resonant surface magnetic x-ray-diffraction measurements performed on the surface of a (111) Co_3Pt alloy, Ferrer *et al.*[42] found that the magnetic moment of the Pt atoms on the first atomic layer was twice smaller than those in the buried layers. This result was attributed to the fact that Pt naturally tends to segregate at surface.

V. SUMMARY AND CONCLUSION

We have performed angle-dependent XMCD experiments at the Co and Pt $L_{2,3}$ edges in two epitaxial (111) $CoPt_3$ thin films in which the appearance of strong perpendicular magnetic anisotropy was clearly related to anisotropic chemical order effects.[6]

For the film grown at 690 K, we find a large anisotropy of the $3d$ orbital magnetic moment ($m_{orb}^{\perp}-m_{orb}^{//}=0.13\mu_B$), related to the formation of anisotropic structural effects, shown by previous XAFS measurements.[7] For the film grown at 800 K, no sizable variation is found in the $3d$ orbital magnetic moment in agreement with its isotropic $L1_2$-type chemical ordering.

The angular dependence of the Pt orbital magnetic moment supports the idea that $5d$ electrons play a crucial role in the appearance of MCA. For the film grown at 690 K, the m_{orb}/m_{spin} ratio is found equal to 0.26 and 0.18 for $\gamma=10°$ and $\gamma=60°$, respectively, while in the film grown at 800 K, this ratio increases slightly with the incidence angle.

ACKNOWLEDGMENTS

We are grateful to D. Stoeffler for calculating the number of Co, Pt, and Au holes in the *d* shells, A. Herr and R. Poinsot for the magnetization measurements, G. Schmerber for the preparation of the $CuAu_3$ bulk alloy, and J. Arabski for the MBE growth of the samples.

[1] W.B. Zeper, F.J.A.M. Greidanus, P.F. Garcia, and C.R. Fincher, J. Appl. Phys. **65**, 4971 (1989).

[2] S. Hashimoto, Y. Ochiai, and K. Aso, J. Appl. Phys. **67**, 2136 (1990).

[3] S.-C. Shin, Appl. Surf. Sci. **65/66**, 110 (1993).

[4] D. Weller, H. Brändle, G. Gorman, C.-J. Lin, and H. Notarys, Appl. Phys. Lett. **61**, 2726 (1992).

[5] P.W. Rooney, A.L. Shapiro, M.Q. Tran, and F. Hellman, Phys. Rev. Lett. **75**, 1843 (1995).

[6] M. Maret, M.C. Cadeville, R. Poinsot, A. Herr, E. Beaurepaire, and C. Monier, J. Magn. Magn. Mater. **166**, 45 (1997).

[7] C. Meneghini, M. Maret, M.C. Cadeville, and J.L. Hazemann, J. Phys. IV Colloq. **7**, C2-1115 (1997).

[8] C. Meneghini, M. Maret, V. Parasote, M.C. Cadeville, J.L. Haze-

mann, R. Cortes, and S. Colonna (unpublished).
[9] D. Weller, J. Stöhr, R. Nakajima, A. Carl, M.G. Samant, C. Chappert, R. Mégy, P. Beauvillain, P. Veillet, and G.A. Held, Phys. Rev. Lett. **75**, 3752 (1995).
[10] P. Bruno, Phys. Rev. B **39**, 865 (1989).
[11] G. van der Laan, J. Phys.: Condens. Matter **10**, 3239 (1998).
[12] B.T. Thole, P. Carra, F. Sette, and G. van der Laan, Phys. Rev. Lett. **68**, 1943 (1992).
[13] P. Carra, B.T. Thole, M. Altarelli, and X. Wang, Phys. Rev. Lett. **70**, 694 (1993).
[14] J. Goulon, N.B. Brookes, C. Gauthier, J.B. Goedkoop, C. Goulon-Ginet, M. Hagelstein, and A. Rogalev, Physica B **208&209**, 199 (1995).
[15] N. Drescher, G. Snell, U. Kleineberg, H.-J. Stock, N. Müller, U. Heinzmann, and N.B. Brookes, Rev. Sci. Instrum. **68**, 1939 (1997).
[16] J. Goulon, C. Goulon-Ginet, R. Cortes, and J.M. Dubois, J. Phys. (Paris) **43**, 539 (1982).
[17] W. Gudat and C. Kunz, Phys. Rev. Lett. **29**, 169 (1972).
[18] S. Eisebitt, T. Böske, J.-E. Rubensson, and W. Eberhardt, Phys. Rev. B **47**, 14 103 (1993).
[19] J. Vogel and M. Sacchi, Phys. Rev. B **49**, 3230 (1994).
[20] W.L. O'Brien and B.P. Tonner, Phys. Rev. B **50**, 12 672 (1994).
[21] F.M.F. de Groot, M.-A. Arrio, Ph. Sainctavit, Ch. Cartier, and C.T. Chen, Solid State Commun. **92**, 991 (1994).
[22] C. Brouder and J.-P. Kappler, in *Magnetism and Synchrotron Radiation*, edited by E. Beaurepaire, B. Carrière, and J.-P. Kappler (Les Editions de Physique, Paris, 1996).
[23] D. Arvanitis, M. Tischer, J. Hunter Dunn, F. May, N. Martensson, and K. Baberschke, in *Spin-Orbit Influenced Spectroscopies of Magnetic Solids*, edited by H. Ebert and G. Schütz (Sringer-Verlag, Berlin, 1996).
[24] D. Stoeffler (private communication). The number of holes in the d shell have been calculated using the augmented spherical wave method for a $CoPt_3$ ($n_h^{3d}=2.25$, $n_h^{5d}=1.80$) and an Au ($n_h^{5d}=0.74$) bulk sample. Note that the change in $5d$ hole counts relative to pure Au for a $CuAu_3$ alloy is lower than 0.03: M. Kuhn and T.K. Sham, Phys. Rev. B **49**, 1647 (1994).
[25] The large perpendicular anisotropy of the orbital magnetic moment exceeds the dipolar energy that tends to redirect the spin magnetic moment in the film plane, yielding the formation of perpendicular alternatively up and down stripe domains in the demagnetized state.
[26] D. Wang, R. Wu, and A.J. Freeman, J. Magn. Magn. Mater. **129**, 237 (1994).
[27] J. Stöhr, J. Electron Spectrosc. Relat. Phenom. **75**, 253 (1995).
[28] Note that the spin magnetic moment is isotropic per definition.
[29] R. Wu and A.J. Freeman, Phys. Rev. Lett. **73**, 1994 (1994).
[30] C.T. Chen, Y.U. Idzerda, H.-J. Lin, N.V. Smith, G. Meigs, E. Chaban, G.H. Ho, E. Pellegrin, and F. Sette, Phys. Rev. Lett. **75**, 152 (1995).
[31] J. Stöhr and H. König, Phys. Rev. Lett. **75**, 3748 (1995).
[32] J.L. Rodríguez-López, J. Dorantes-Dávila, and G.M. Pastor, Phys. Rev. B **57**, 1040 (1998).
[33] G.H.O. Daalderop, P.J. Kelly, and M.F.H. Schuurmans, Phys. Rev. B **50**, 9989 (1994).
[34] I.V. Solovyev, P.H. Dederichs, and I. Mertig, Phys. Rev. B **52**, 13 419 (1995).
[35] G. Shütz, M. Knülle, R. Wienke, W. Wihlem, W. Wagner, P. Kienle, R. Zeller, and R. Frahm, Z. Phys. B **75**, 495 (1989).
[36] H. Maruyama, F. Matsuoka, K. Kobayashi, and H. Yamazaki, Physica B **208&209**, 787 (1995).
[37] H. Maruyama, F. Matsuoka, K. Kobayashi, and H. Yamazaki, J. Magn. Magn. Mater. **140-144**, 43 (1995).
[38] L.F. Mattheiss and R.E. Dietz, Phys. Rev. B **22**, 1663 (1980).
[39] J. Vogel, A. Fontaine, V. Cros, F. Petroff, J.-P. Kappler, G. Krill, A. Rogalev, and J. Goulon, Phys. Rev. B **55**, 3663 (1997).
[40] C.J. Talnall, J.P. Schillé, P.J. Grundy, and D.G. Lord, J. Magn. Magn. Mater. **165**, 391 (1997).
[41] H. Ebert, S. Ruegg, G. Schütz, R. Wienke, and W.B. Zeper, J. Magn. Magn. Mater. **93**, 601 (1991).
[42] S. Ferrer, P. Fajardo, F. de Bergevin, J. Alvarez, X. Torreles, H.A. van der Vegt, and V.H. Etgens, Phys. Rev. Lett. **77**, 747 (1996).